

New nonuniform black string solutions

Burkhard Kleihaus^{1*}, Jutta Kunz^{1†} and Eugen Radu^{2‡}

¹*Institut für Physik, Universität Oldenburg, Postfach 2503 D-26111 Oldenburg, Germany*

²*Department of Mathematical Physics, National University of Ireland, Maynooth, Ireland*

ABSTRACT: We present nonuniform vacuum black strings in five and six spacetime dimensions. The conserved charges and the action of these solutions are computed by employing a quasilocal formalism. We find qualitative agreement of the physical properties of nonuniform black strings in five and six dimensions. Our results offer further evidence that the black hole and the black string branches merge at a topology changing transition. We generate black string solutions of the Einstein-Maxwell-dilaton theory by using a Harrison transformation. We argue that the basic features of these solutions can be derived from those of the vacuum black string configurations.

KEYWORDS: black strings, numerical solutions, Harrison transformation.

*E-mail: kleihaus@theorie.physik.uni-oldenburg.de

†E-mail: kunz@theorie.physik.uni-oldenburg.de

‡E-mail: radu@thphys.nuim.ie

Contents

1. Introduction	1
2. General ansatz and properties of the solutions	2
2.1 The equations and boundary conditions	2
2.2 Properties of the solutions	4
2.3 A counterterm approach	6
2.4 Remarks on nonuniform bubble-like solutions	7
3. Numerical nonuniform black string solutions	8
3.1 Numerical procedure	8
3.2 Black string properties	9
3.3 Black strings and black holes	16
4. Black string solutions in Einstein-Maxwell-dilaton theory	20
4.1 Asymptotically $\mathcal{M}^{D-1} \times S^1$ EMD black string solutions	21
4.2 Black strings in a background magnetic field	23
5. Conclusions	25
A. Appendix	27

1. Introduction

In recent years it has been realized that, even at the classical level, gravity exhibits a much richer structure in higher dimensions than in four dimensions.

Black string solutions, present for $D \geq 5$ spacetime dimensions, are of particular interest, since they exhibit new features that have no analogue in the black hole case. Such configurations are important if one supposes the existence of extradimensions in the universe, which are likely to be compact and described by a Kaluza-Klein (KK) theory.

The simplest vacuum static solution of this type is found by assuming translational symmetry along the extracordinate direction, and corresponds to a uniform black string with horizon topology $S^{D-3} \times S^1$. Although this solution exists for all values of the mass, it is unstable below a critical value as shown by Gregory and Laflamme [1]. This instability was interpreted to mean that a light uniform string decays to a black hole since that has higher entropy. However, Horowitz and Maeda [2] argued that the horizon could not pinch off, so

the end state of the instability could not be a collection of separate black holes. Instead, they conjectured that the solution would settle down to a non-translationally invariant solution with the same horizon topology as the original configuration.

This prompted a search for this missing link, and a branch of static nonuniform black string solutions was subsequently found by perturbing the uniform black string by the threshold unstable mode. The $D = 5$ approximate solutions were obtained in [3], perturbed $D = 6$ were presented in [4], and higher dimensional generalizations were discussed in [5].

Despite some attempts, no analytic solutions are available for nonuniform black string solutions and one has to employ numerical techniques. At present, the nonuniform branch is numerically known only for $D = 6$ [4] (see also the post-analysis in [6], [7]).

Apart from the black string solutions, KK theory possesses also a branch of black hole solutions with an event horizon of topology S^{D-2} . The numerical results presented in [8] (following a conjecture put forward in [9]) suggest that, at least for $D = 6$, the black hole and the nonuniform string branches merge at a topology changing transition. Still, a number of aspects remain to be clarified, and the literature on nonuniform black string and black hole solutions in KK theory is continuously growing (see [10, 11] for recent reviews).

The main purpose of this paper is to numerically construct and study the nonuniform black string branch in $D = 5$. This dimension is of particular interest since one may join the black string results with those of the $D = 5$ black hole branch discussed in [8] (see also [12]).

We begin with a presentation of the general ansatz and the relevant quantities for an arbitrary spacetime dimension D . In this context, we propose to compute the mass, tension and action of the nonuniform black string solutions by using a quasilocal formalism. In Section 3 we present our numerical results. We demonstrate that for $D = 5$ a branch of nonuniform black string solutions exists, at least within the scope of our numerical approximation. The numerical methods used here are rather different from the methods employed to obtain the $D = 6$ solutions [4]. We construct nonuniform black string solutions also in $D = 6$ dimensions, extending the known set of solutions [4] to larger deformation of the event horizon. In Section 4 solutions of the Einstein-Maxwell-dilaton (EMD) equations are generated from the vacuum configurations, by using a Harrison transformation originally derived in [13]. The basic properties of two different types of solutions, corresponding to charged black strings which asymptote to $\mathcal{M}^{D-1} \times S^1$ and black strings in a background magnetic field are discussed there. We give our conclusions and remarks in the final section. The Appendix contains a brief discussion of some numerical aspects of our solutions.

2. General ansatz and properties of the solutions

2.1 The equations and boundary conditions

We consider the Einstein action

$$I = \frac{1}{16\pi G} \int_M d^D x \sqrt{-g} R - \frac{1}{8\pi G} \int_{\partial M} d^{D-1} x \sqrt{-h} K, \quad (2.1)$$

in a D -dimensional spacetime. The last term in (2.1) is the Hawking-Gibbons surface term [14], which is required in order to have a well-defined variational principle. K is the trace of the extrinsic curvature for the boundary $\partial\mathcal{M}$ and h is the induced metric of the boundary.

We consider black string solutions approaching asymptotically the $D - 1$ dimensional Minkowski-space times a circle $\mathcal{M}^{D-1} \times S^1$. We denote the compact direction as $z = x^{D-1}$ and the directions of R^{D-2} as x^1, \dots, x^{D-2} , while $x^D = t$. The direction z is periodic with period L . We also define the radial coordinate r by $r^2 = (x^1)^2 + \dots + (x^{D-2})^2$.

The nonuniform black string solutions presented in this paper are found within the metric ansatz ¹

$$ds^2 = -e^{2A(r,z)} f(r) dt^2 + e^{2B(r,z)} \left(\frac{dr^2}{f(r)} + dz^2 \right) + e^{2C(r,z)} r^2 d\Omega_{D-3}^2, \quad (2.2)$$

where

$$f = 1 - \left(\frac{r_0}{r} \right)^{D-4}.$$

The Einstein equations $G_t^t = 0$, $G_r^r + G_z^z = 0$ and $G_\theta^\theta = 0$ (where θ denotes an angle of the $D - 3$ dimensional sphere) then yield for the functions A , B , C the set of equations [4]

$$\begin{aligned} A'' + \frac{\ddot{A}}{f} + A'^2 + \frac{\dot{A}^2}{f} + (D-3) \left(A'C' + \frac{\dot{A}\dot{C}}{f} + \frac{A'}{r} + \frac{f'C'}{2f} + \frac{f'}{2rf} \right) + \frac{f''}{2f} + \frac{3f'A'}{2f} &= 0, \\ B'' + \frac{\ddot{B}}{f} + \frac{(D-3)(D-4)}{2r^2} \left(-1 + \frac{e^{2B-2C}}{f} - \frac{r^2\dot{C}^2}{f} - 2rC' - r^2C'^2 \right) & \\ - (D-3) \left(\frac{f'}{2rf} + \frac{\dot{A}\dot{C}}{f} + \frac{A'}{r} + \frac{f'C'}{2f} + A'C' \right) + \frac{f'B'}{2f} &= 0, \\ C'' + \frac{\ddot{C}}{f} + (D-3) \left(C'^2 + \frac{\dot{C}^2}{f} + \frac{2C'}{r} \right) + \frac{(D-4)}{r^2} \left(1 - \frac{e^{2B-2C}}{f} \right) & \\ + \frac{f'}{rf} + \frac{\dot{A}\dot{C} + f'C'}{f} + \frac{A'}{r} + A'C' &= 0, \end{aligned} \quad (2.3)$$

where a prime denotes $\partial/\partial r$, and a dot $\partial/\partial z$.

The remaining Einstein equations $G_z^r = 0$, $G_r^r - G_z^z = 0$ yield two constraints. Following [4], we note that setting $G_t^t = G_\theta^\theta = G_\varphi^\varphi = G_r^r + G_z^z = 0$ in $\nabla_\mu G^{\mu r} = 0$ and $\nabla_\mu G^{\mu z} = 0$, we obtain

$$\begin{aligned} \partial_z (\sqrt{-g} G_z^r) + \sqrt{f} \partial_r \left(\sqrt{f} \sqrt{-g} \frac{1}{2} (G_r^r - G_z^z) \right) &= 0, \\ \sqrt{f} \partial_r (\sqrt{-g} G_z^r) - \partial_z \left(\sqrt{f} \sqrt{-g} \frac{1}{2} (G_r^r - G_z^z) \right) &= 0, \end{aligned} \quad (2.4)$$

¹An ansatz involving only two undetermined functions was suggested in [15] for a special coordinate choice. However, we could not obtain numerical solutions of the Einstein equations within that reduced ansatz.

and, defining \hat{r} via $\partial/\partial\hat{r} = \sqrt{f}\partial/\partial r$, then yields the Cauchy-Riemann relations

$$\begin{aligned}\partial_z(\sqrt{-g}G_z^r) + \partial_{\hat{r}}\left(\sqrt{f}\sqrt{-g}\frac{1}{2}(G_r^r - G_z^z)\right) &= 0, \\ \partial_{\hat{r}}(\sqrt{-g}G_z^r) - \partial_z\left(\sqrt{f}\sqrt{-g}\frac{1}{2}(G_r^r - G_z^z)\right) &= 0.\end{aligned}\tag{2.5}$$

Thus the weighted constraints satisfy Laplace equations, and the constraints are fulfilled, when one of them is satisfied on the boundary and the other at a single point [4].

The event horizon resides at a surface of constant radial coordinate $r = r_0$ and is characterized by the condition $f(r_0) = 0$. Introducing the coordinate \tilde{r} , where $r = \sqrt{r_0^2 + \tilde{r}^2}$, the horizon resides at $\tilde{r} = 0$.

Utilizing the reflection symmetry of the nonuniform black strings w.r.t. $z = L/2$, the solutions are constructed subject to the following set of boundary conditions

$$A|_{\tilde{r}=\infty} = B|_{\tilde{r}=\infty} = C|_{\tilde{r}=\infty} = 0,\tag{2.6}$$

$$A|_{\tilde{r}=0} - B|_{\tilde{r}=0} = d_0, \quad \partial_{\tilde{r}}A|_{\tilde{r}=0} = \partial_{\tilde{r}}C|_{\tilde{r}=0} = 0,\tag{2.7}$$

$$\partial_z A|_{z=0,L/2} = \partial_z B|_{z=0,L/2} = \partial_z C|_{z=0,L/2} = 0,\tag{2.8}$$

where the constant d_0 is related to the Hawking temperature of the solutions. Regularity further requires that the condition $\partial_{\tilde{r}}B|_{\tilde{r}=0} = 0$ holds for the solutions. The boundary conditions guarantee, that the constraints are satisfied, since $\sqrt{-g}G_z^r = 0$ everywhere on the boundary, and $\sqrt{f}\sqrt{-g}(G_r^r - G_z^z) = 0$ on the horizon.

2.2 Properties of the solutions

For any static spacetime which is asymptotically $\mathcal{M}^{D-1} \times S^1$ one can define a mass M and a tension \mathcal{T} [16], these quantities being encoded in the asymptotics of the metric potentials. As discussed in [17], [18], the asymptotic form of the relevant metric components of any static solution is

$$g_{tt} \simeq -1 + \frac{c_t}{r^{D-4}}, \quad g_{zz} \simeq 1 + \frac{c_z}{r^{D-4}}.\tag{2.9}$$

When computing M , \mathcal{T} or the gravitational action, the essential idea is to consider the asymptotic values of the gravitational field far away from the black string and to compare them with those corresponding to a gravitational field in the absence of the black string. Therefore, this prescription provides results that are relative to the choice of a reference background, whose obvious choice in our case is $\mathcal{M}^{D-1} \times S^1$.

The mass and tension of black string solutions as computed in [17, 19] are given by

$$M = \frac{\Omega_{D-3}L}{16\pi G}((D-3)c_t - c_z), \quad \mathcal{T} = \frac{\Omega_{D-3}}{16\pi G}(c_t - (D-3)c_z),\tag{2.10}$$

where Ω_{D-3} is the area of the unit S^{D-3} sphere. The corresponding quantities of the uniform string solution M_0 and \mathcal{T}_0 are obtained from (2.10) for $c_z = 0$, $c_t = r_0^{D-4}$. One can also define a relative tension n (also called the relative binding energy or scalar charge)

$$n = \frac{\mathcal{T}L}{M} = \frac{c_t - (D-3)c_z}{(D-3)c_t - c_z}. \quad (2.11)$$

which measures how large the tension is relative to the mass. This dimensionless quantity is bounded, $0 \leq n \leq D-3$. Uniform string solutions have relative tension $n_0 = 1/(D-3)$. Another useful quantity is the rescaled dimensionless mass

$$\mu = \frac{16\pi GM}{L^{D-3}}. \quad (2.12)$$

The Hawking temperature and entropy of the black string solutions are given by

$$T = e^{A_0 - B_0} T_0, \quad S = S_0 \frac{1}{L} \int_0^L e^{B_0 + (D-3)C_0} dz, \quad (2.13)$$

where T_0 , S_0 are the corresponding quantities of the uniform solution

$$T_0 = \frac{D-4}{4\pi r_0}, \quad S_0 = \frac{1}{4} L \Omega_{D-3} r_0^{D-3}, \quad (2.14)$$

and $A_0(z), B_0(z), C_0(z)$ are the values of the metric functions on the event horizon $r = r_0$.

Together with the mass M and relative tension n , these quantities obey the Smarr formula [17]

$$TS = \frac{D-3-n}{D-2} M. \quad (2.15)$$

Note that the relations (2.9)-(2.12) and (2.15) are also valid for black hole solutions.

Black string thermodynamics can be discussed by employing the very general connection between entropy and geometry established in the Euclidean path integral approach to quantum gravity [14]. In this approach, the partition function for the gravitational field is defined by a sum over all smooth Euclidean geometries which are periodic with a period β in imaginary time. This integral is computed by using the saddle point approximation, and the energy and entropy of the solutions are evaluated by standard thermodynamic formulae.

We consider a canonical ensemble with Helmholtz free energy (thus at fixed temperature and extradimension length)

$$F[T, L] = \frac{I}{\beta} = M - TS \quad (2.16)$$

The Euclidean action of the vacuum solutions computed by subtracting the background contribution is

$$I = \frac{1}{16\pi G} \beta \Omega_{D-3} (c_t - c_z) = \frac{\beta}{D-2} (M + \mathcal{T}L), \quad (2.17)$$

with $\beta = 1/T$.

The first law of thermodynamics reads

$$dM = TdS + \mathcal{T}dL. \quad (2.18)$$

It follows that

$$S = - \left(\frac{\partial F}{\partial T} \right)_L, \quad \mathcal{T} = - \left(\frac{\partial F}{\partial L} \right)_T. \quad (2.19)$$

Combining the Smarr formula (2.15) and the first law, it follows that, given a curve $n(\mu)$ in the (n, μ) -plane, the entire thermodynamics can be obtained [17].

We remark also that the Einstein equations (2.3) are left invariant by the transformation $r \rightarrow kr, z \rightarrow kz, r_0 \rightarrow r_0/k$, with k an arbitrary positive integer. Therefore, one may generate a family of vacuum solutions in this way, termed copies of solutions. The new solutions have the same length of the extradimension. Their relevant properties, expressed in terms of the corresponding properties of the initial solution, read

$$M_k = \frac{M}{k^{D-4}}, \quad T_k = kT, \quad S_k = \frac{S}{k^{D-3}}, \quad n_k = n. \quad (2.20)$$

This transformation, suggested first by Horowitz [20], has been discussed in [21] for $D = 6$.

2.3 A counterterm approach

Similar results for the black strings' mass, tension and action are obtained by using the quasilocal tensor of Brown and York [22], augmented by the counterterms formalism. This technique consists in adding suitable counterterms I_{ct} to the action of the theory. These counterterms are built up with curvature invariants of the induced metric on the boundary $\partial\mathcal{M}$ (which is sent to infinity after the integration) and thus obviously they do not alter the bulk equations of motion. By choosing appropriate counterterms which cancel the divergencies, one can then obtain well-defined expressions for the action and the energy momentum of the spacetime. Unlike the background subtraction, this procedure is satisfying since it is intrinsic to the spacetime of interest and it is unambiguous once the counterterm is specified. While there is a general algorithm to generate the counterterms for asymptotically (anti-)de Sitter spacetimes, the asymptotically flat case is less-explored (see however [23] and the more general approach in recent work [24]).

It is also important to note that the counterterm method gives results that are equivalent to what one obtains using the background subtraction method. However, we employ it because it appears to be a more general technique than background subtraction, and it is interesting to explore the range of problems to which it applies.

Therefore, we add the following counterterm part to the action principle (2.1)

$$I_{ct} = -\frac{1}{8\pi G} \int_{\partial\mathcal{M}} d^{D-1}x \sqrt{-h} \sqrt{\frac{D-3}{D-4}} \mathcal{R}, \quad (2.21)$$

where \mathcal{R} is the Ricci scalar of the boundary geometry.

Varying the total action with respect to the boundary metric h_{ij} , we compute the boundary stress-tensor

$$T_{ij} = \frac{2}{\sqrt{-h}} \frac{\delta I}{\delta h^{ij}} = \frac{1}{8\pi G} \left(K_{ij} - h_{ij} K - \Psi (\mathcal{R}_{ij} - \mathcal{R} h_{ij}) - h_{ij} \square \Psi + \Psi_{;ij} \right), \quad (2.22)$$

where K_{ij} is the extrinsic curvature of the boundary and $\Psi = \sqrt{\frac{D-3}{(D-4)\mathcal{R}}}$.

Provided the boundary geometry has an isometry generated by a Killing vector ξ^i , a conserved charge

$$\mathcal{Q}_\xi = \oint_\Sigma d^{D-2} S^i \xi^j T_{ij} \quad (2.23)$$

can be associated with a closed surface Σ . Physically, this means that a collection of observers on the boundary with the induced metric h_{ij} measure the same value of \mathcal{Q}_ξ .

The mass and tension are the charges associated to $\partial/\partial t$ and $\partial/\partial z$, respectively (note that $\partial/\partial z$ is a Killing symmetry of the boundary metric). The relevant components of the boundary stress tensor are

$$T_t^t = \frac{1}{16\pi G} \frac{(D-3)c_t - c_z}{r^{D-3}} + O(1/r^{D-2}), \quad T_z^z = \frac{1}{16\pi G} \frac{c_t - (D-3)c_z}{r^{D-3}} + O(1/r^{D-2}). \quad (2.24)$$

The mass and tension computed from (2.23) agree with the expressions (2.10)².

One should remark that the counterterm choice is not unique, other choices being possible as well (see [25] for a related discussion). Our choice of using (2.21) was motivated by the fact that the general expression for the boundary stress-tensor is very simple. For an asymptotically $\mathcal{M}^{D-1} \times S^1$ spacetime, we find that I_{ct} (2.21) or other possible choices proposed in [23] regularizes also the black strings Euclidean action, yielding similar results to those obtained within the background subtraction approach.

2.4 Remarks on nonuniform bubble-like solutions

There is also a simple way to generate time dependent solutions with a nontrivial extradiimension dependence. A Lorentzian solution of the vacuum Einstein equations is found by using the following analytic continuation in the general configuration (2.2) (with $d\Omega_{D-3}^2 = d\theta^2 + \sin^2 \theta d\Omega_{D-4}^2$)

$$t \equiv i\chi, \quad \theta - \pi/2 \equiv i\tau. \quad (2.25)$$

The new solution reads

$$ds^2 = e^{2A(r,z)} f(r) d\chi^2 + e^{2B(r,z)} \left(\frac{dr^2}{f(r)} + dz^2 \right) + e^{2C(r,z)} r^2 (-d\tau^2 + \cosh^2 \tau d\Omega_{D-4}^2), \quad (2.26)$$

²Note that in computing \mathcal{T} , one should consider the integration over $\hat{S}^z = S^z/\Delta t$, with $\Delta t = \int dt$. However, a similar problem appears also in the Hamiltonian approach [19].

with $A(r, z)$, $B(r, z)$, $C(r, z)$ and $f(r)$ the functions of the black string configuration.

This technique of double analytic continuation was originally developed for the study of the stability of the KK vacuum [26], [27], and has been considered in the last years by many authors in AdS/CFT context (see e.g. [28]).

However, the solution one finds starting with a nonuniform vacuum black string has some new features, as compared to the Schwarzschild-Tangherlini seed solution. In that case, the resulting spacetime describes a contracting and then expanding "bubble of nothing". The new configuration (2.26) has now two compact extradimensions z and χ . The radial variable r is restricted to the range $r \geq r_0$. $r = r_0$ is not the boundary of spacetime, but it is the $S^{D-4} \times S^1$ of minimal area. The curves at $r = r_0$ with constant z (and constant points on S^{D-4}) are geodesics. Also, regularity at $r = r_0$ requires χ to be periodic with period $\beta = 1/T$, with T given by (2.13). One can see that the geometry traced out by the $r = r_0$ surface is the $(D - 3)$ -dimensional de Sitter spacetime with a z -dependent conformal factor, times the extradimension. Thus (2.26) would rather describe a nonuniform "vortex of nothing".

One can use the same techniques as in Section 4 to find the corresponding D -dimensional solutions in Einstein-Maxwell-dilaton theory.

KK bubble solutions in $d = 5, 6$ dimensions have been also considered in Ref. [29]. A number of exact solutions have been presented there, describing sequences of KK bubbles and black holes, placed alternately so that the black holes are held apart by the bubbles. However, the configurations in [29] differ from (2.26), since they are static and asymptotically approach Minkowski spacetime times a circle.

3. Numerical nonuniform black string solutions

3.1 Numerical procedure

Our main concern here is the numerical construction of nonuniform black string solutions in $D = 5$ dimensions. We have also constructed nonuniform black string solutions in $D = 6$ dimensions, reproducing and extending the known set of solutions, obtained previously by different methods, which could not be successfully applied in $D = 5$ dimensions [4, 6, 7, 8].

To obtain nonuniform black string solutions, we solve the set of three coupled non-linear elliptic partial differential equations numerically [30], subject to the above boundary conditions. We employ dimensionless coordinates \bar{r} and \bar{z} ,

$$\bar{r} = \tilde{r}/(1 + \tilde{r}), \quad \bar{z} = z/L, \tag{3.1}$$

where the compactified radial coordinate \bar{r} maps spatial infinity to the finite value $\bar{r} = 1$, and L is the asymptotic length of the compact direction. The numerical calculations are based on the Newton-Raphson method and are performed with help of the program FIDISOL [30], which provides also an error estimate for each unknown function.

The equations are discretized on a non-equidistant grid in \bar{r} and \bar{z} . Typical grids used have sizes 65×50 , covering the integration region $0 \leq \bar{r} \leq 1$ and $0 \leq \bar{z} \leq 1/2$. (See [30])

and [31] for further details and examples for the numerical procedure.) For the nonuniform strings the estimated relative errors range from approximately $\approx 0.001\%$ for small geometric deformation to $\approx 1\%$ for large deformation. Further discussion of the numerical accuracy is deferred to Appendix A.

The horizon coordinate r_0 and the asymptotic length L of the compact direction enter the equations of motion as parameters. The results presented are mainly obtained with the parameter choice

$$r_0 = 1, \quad L = L^{\text{crit}} = \begin{cases} 7.1713 & D = 5 \\ 4.9516 & D = 6 \end{cases}, \quad (3.2)$$

where L^{crit} represents the value, where the instability of the uniform string occurs. The branch of nonuniform strings is then obtained by starting at the critical point of the uniform string branch and varying the boundary parameter d_0 , which enters the Eq. (2.7), relating the values of the functions A and B at the horizon.

3.2 Black string properties

Let us first consider the metric functions A , B and C for nonuniform string solutions as functions of the radial coordinate r and of the coordinate z of the compact direction. Keeping the asymptotic length L of the compact direction and the horizon coordinate r_0 fixed, the solutions change smoothly with boundary parameter d_0 . A measure of the deformation of the solutions is given by the nonuniformity parameter λ [3]

$$\lambda = \frac{1}{2} \left(\frac{\mathcal{R}_{\text{max}}}{\mathcal{R}_{\text{min}}} - 1 \right), \quad (3.3)$$

where \mathcal{R}_{max} and \mathcal{R}_{min} represent the maximum radius of a $(D-3)$ -sphere on the horizon and the minimum radius, being the radius of the ‘waist’. Thus for uniform black strings $\lambda = 0$, while the conjectured horizon topology changing transition should be approached for $\lambda \rightarrow \infty$ [7, 6]. As d_0 first increases and then decreases again, the nonuniformity parameter λ increases monotonically.

In Figure 1 we exhibit the metric functions for $D = 5$ nonuniform string solutions for several values of the nonuniformity parameter, $\lambda = 1, 2, 5, 9$. The functions exhibit extrema on the symmetry axis $z = 0$ at the horizon. As λ increases, the extrema increase in height and become increasingly sharp (implying a deteriorating numerical accuracy for large values of λ).

To obtain a more quantitative picture of the metric functions, we exhibit $-g_{tt}/f = e^{2A}$, $g_{zz} = e^{2B}$, and $g_{\theta\theta}/r^2 = e^{2C}$ in Figure 2 for several fixed values of z .

The spatial embedding of the horizon into 3-dimensional space is shown in Figure 3 for the $D = 5$ nonuniform black string solutions. In these embeddings the proper radius of the horizon is plotted against the proper length along the compact direction, yielding a geometrical view of the nonuniformity of the solutions.

The deformation of the horizon of the $D = 5$ nonuniform black string solutions is further explored in Figure 4. The maximum radius of the 2-sphere on the horizon \mathcal{R}_{max} and the

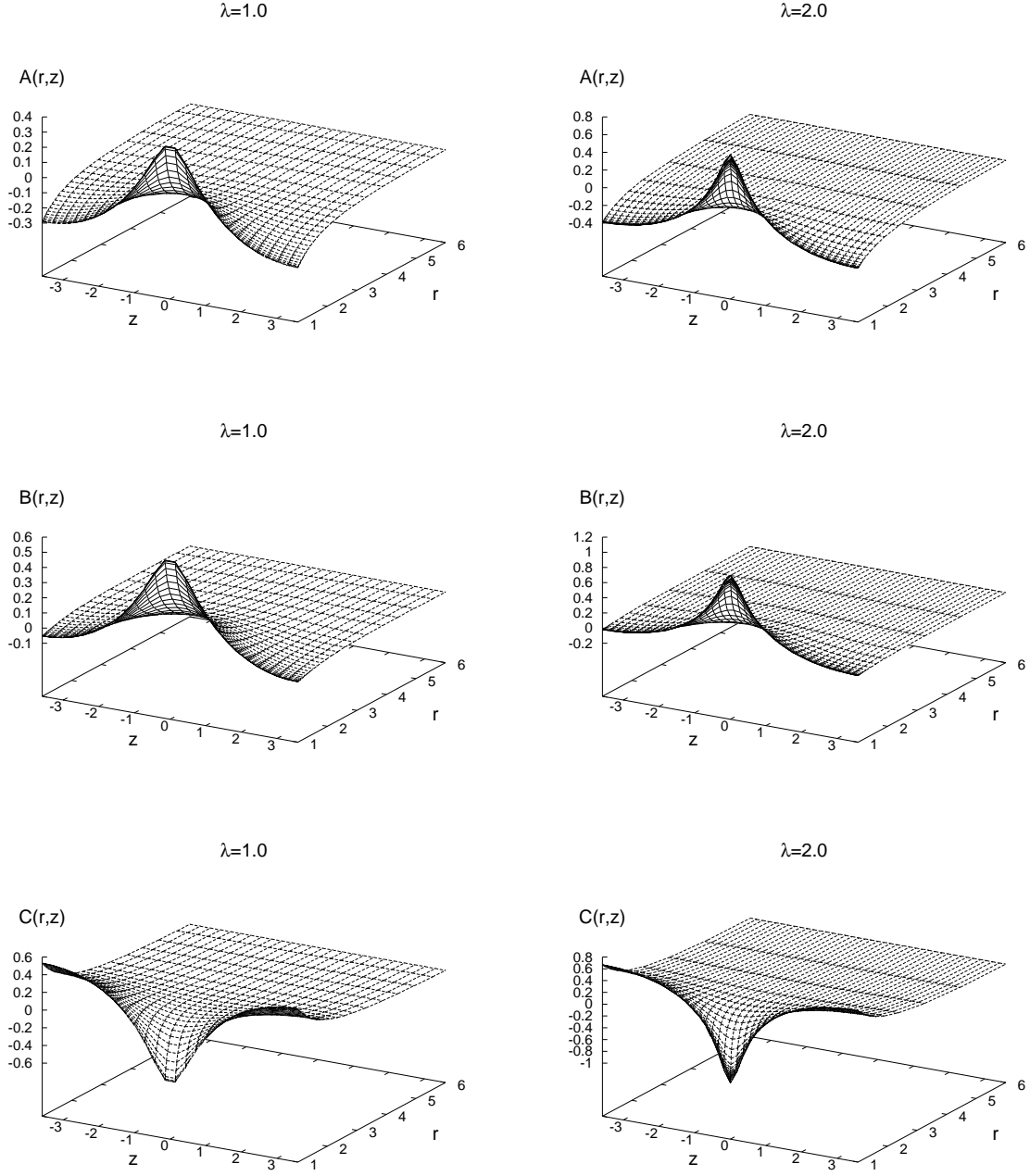


Figure 1. The metric functions A , B and C of the $D = 5$ nonuniform string solutions are shown as functions of the radial coordinate r , with the horizon located at $r_0 = 1$, and the coordinate z of the compact direction with asymptotic length $L = L^{\text{crit}} = 7.1713$, for several values of the nonuniformity parameter, $\lambda = 1$ (first column), $\lambda = 2$ (second column), $\lambda = 5$ (third column), $\lambda = 9$ (fourth column).

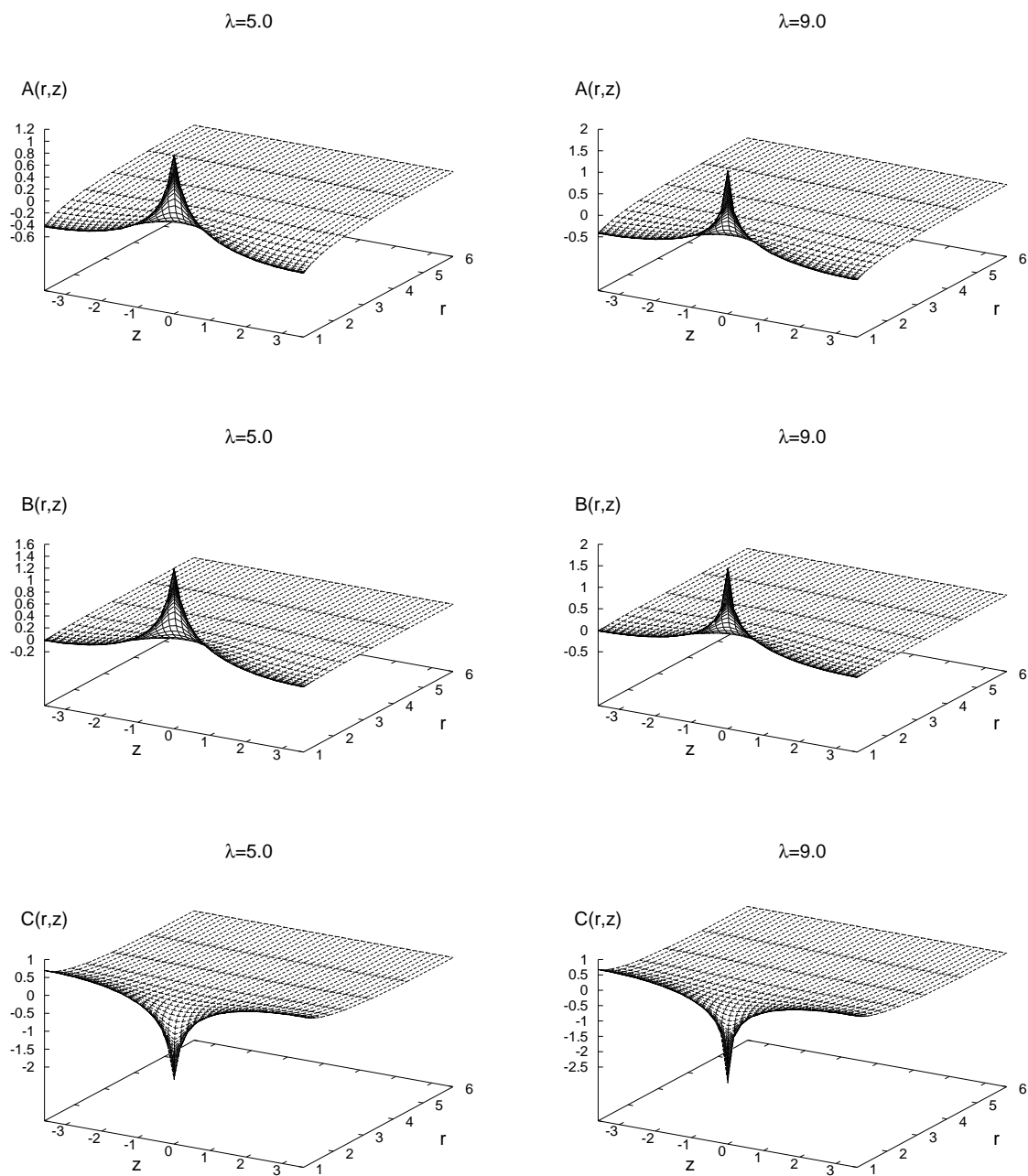


Figure 1. Figure 1 continued.

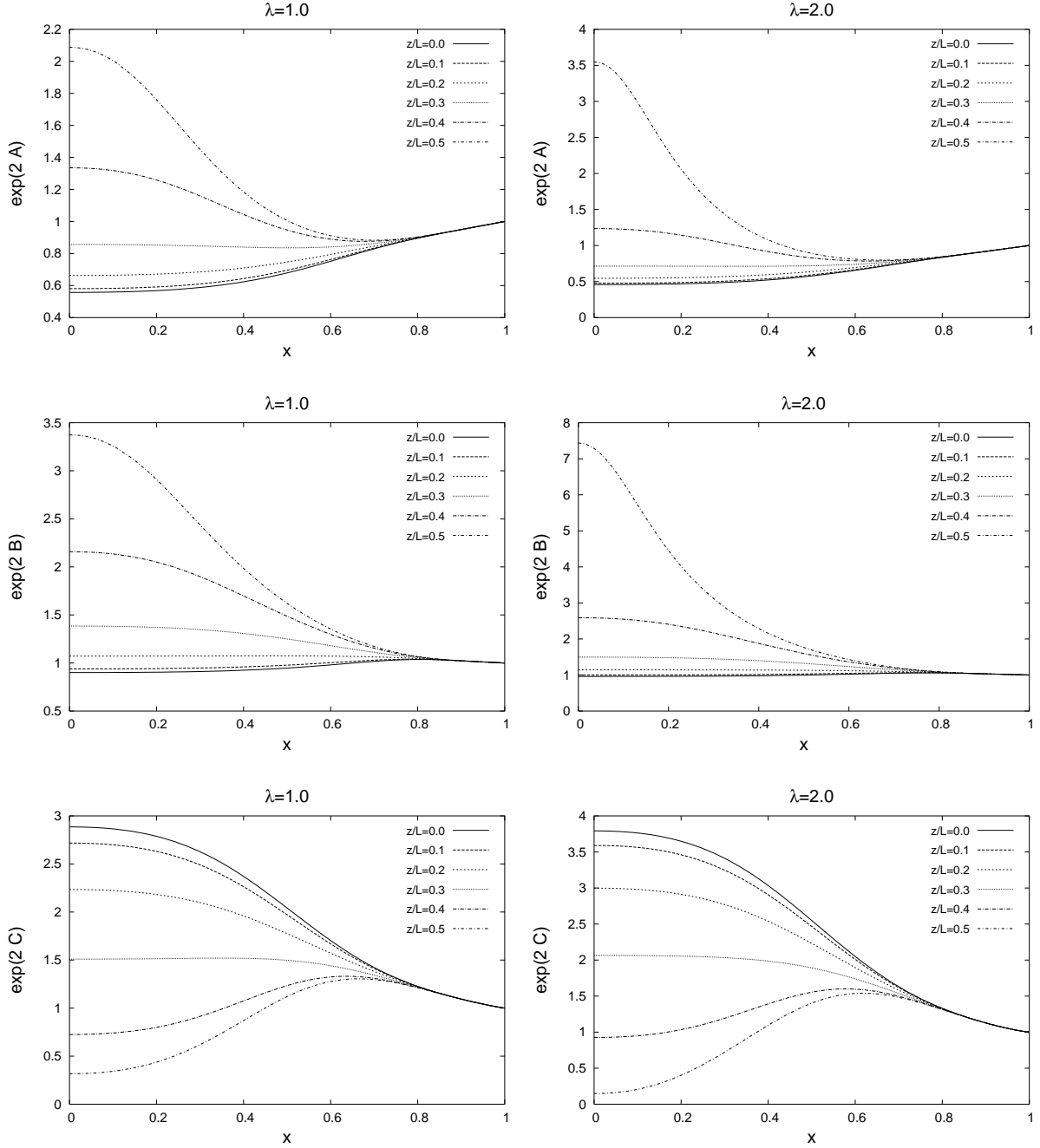


Figure 2. The metric functions e^{2A} , e^{2B} , and e^{2C} of the $D = 5$ nonuniform string solutions are shown as functions of the compactified radial coordinate $x = \bar{r}$, for several fixed values of the coordinate z of the compact direction ($z/L = 0, 0.1, 0.2, 0.3, 0.4, 0.5$), as well as of the nonuniformity parameter λ ($\lambda = 1$ (first column), $\lambda = 2$ (second column), $\lambda = 5$ (third column), $\lambda = 9$ (fourth column)).

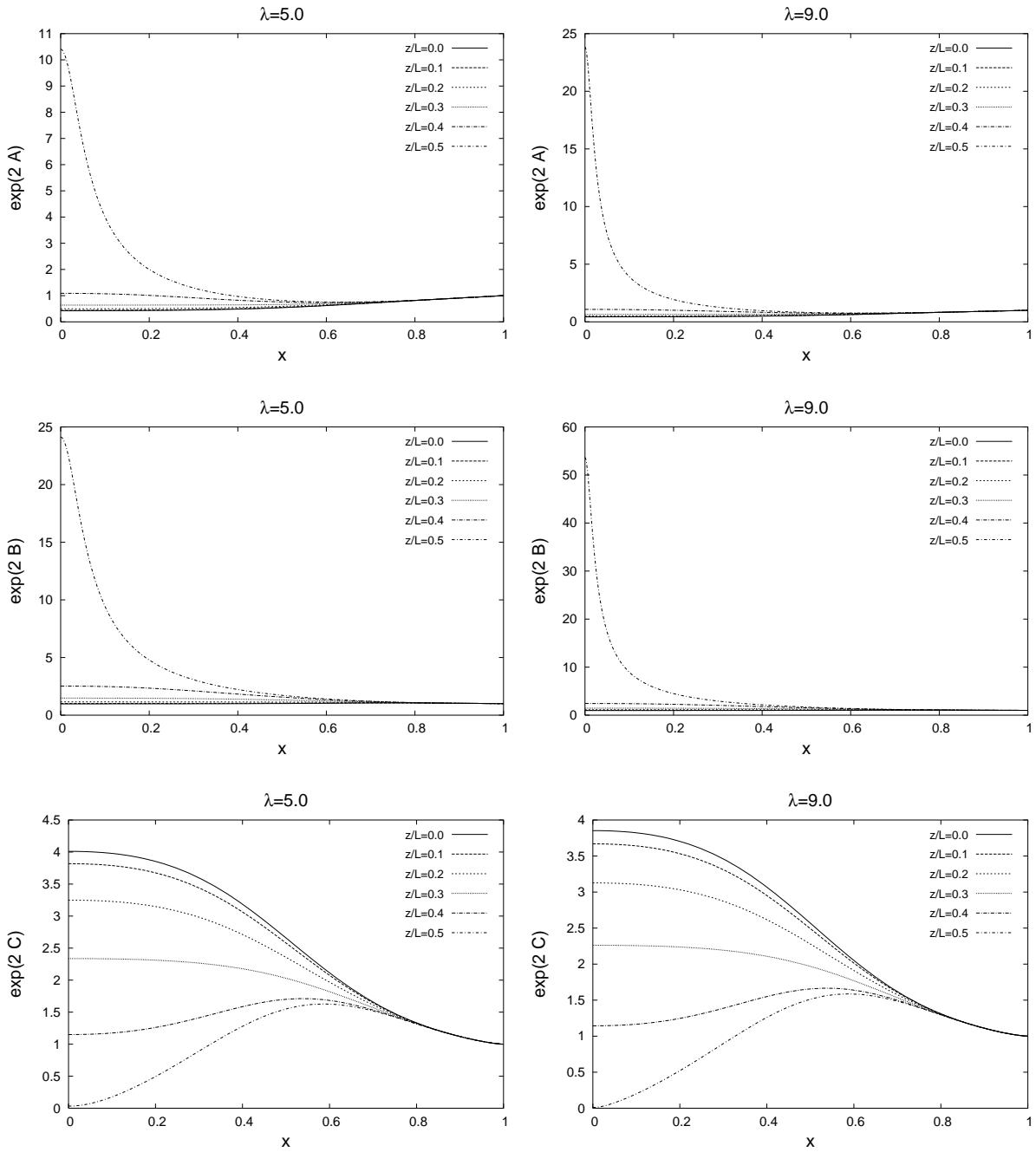


Figure 2. Figure 2 continued.

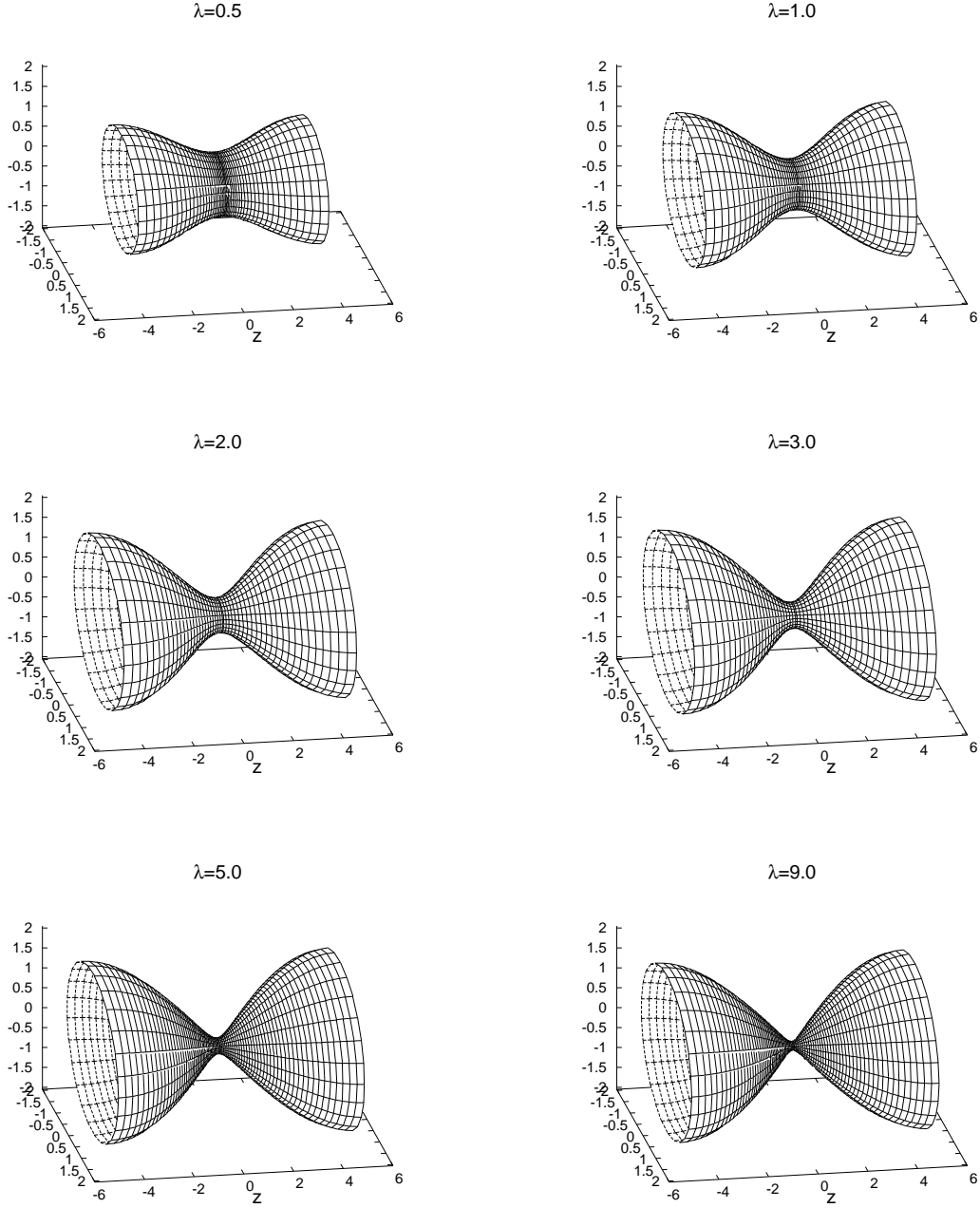


Figure 3. The spatial embedding of the horizon of $D = 5$ nonuniform black string solutions with horizon coordinate $r_0 = 1$ and asymptotic length of the compact direction $L = L^{\text{crit}} = 7.1713$, is shown for several values of the nonuniformity parameter, $\lambda = 0.5, 1, 2, 3, 5, 9$.

minimum radius \mathcal{R}_{\min} representing the ‘waist’ are presented together with the proper length L_H of the horizon along the compact direction as functions of the nonuniformity parameter λ , ranging from $0 \leq \lambda \leq 9$.

With increasing λ , \mathcal{R}_{\max} first increases, reaches a maximum around $\lambda \approx 4$ and then decreases slightly again towards still larger values of the nonuniformity parameter; in contrast L_H/L increases monotonically and \mathcal{R}_{\min} decreases monotonically (in the range considered). We expect that \mathcal{R}_{\max} and L_H/L approach finite values in the limit $\lambda \rightarrow \infty$, whereas \mathcal{R}_{\min} should reach zero in this limit, when extrapolated (approximately linearly) in the figure. For comparison, we also show in the figure the corresponding geometric quantities of the $D = 6$ nonuniform black string solutions.

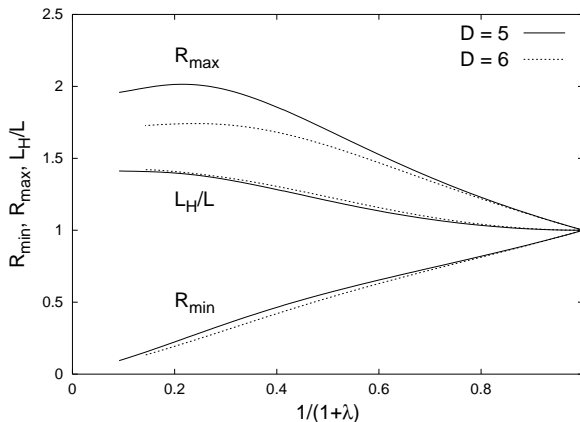


Figure 4. The maximum radius of the $(D-3)$ -sphere on the horizon \mathcal{R}_{\max} , the minimum radius \mathcal{R}_{\min} , and the proper length L_H of the horizon along the compact direction divided by the asymptotic length $L = L^{\text{crit}}$ are shown for $D = 5$ and $D = 6$ nonuniform black string solutions as functions of $1/(1+\lambda)$.

We exhibit in Figure 5 the mass M , the relative tension n , the temperature T and the entropy S of the $D = 5$ and $D = 6$ nonuniform string solutions, in units of the corresponding uniform string solution, versus the nonuniformity parameter λ . Interestingly, the mass and the entropy assume a maximal value in the vicinity of $\lambda \approx 4$, while the tension and the temperature assume a minimal value, both in 5 and in 6 dimensions. Since the extrema appear only around $\lambda \approx 4$, which is the maximal value of λ obtained in previous calculations [6], they were not recognized there. Extrapolating these quantities to $\lambda \rightarrow \infty$ yields for the tension the critical value n_* , where $n_*/n_0 \approx 0.8$ for $D = 5$ and $n_*/n_0 \approx 0.6$ in six spacetime dimensions.

The mass and tension exhibited in Figure 5 are obtained from the 1st law of thermodynamics together with the Smarr relation (2.15). A discussion of the mass and the string tension as obtained from the asymptotic fall-off of the metric functions is given in Appendix A.

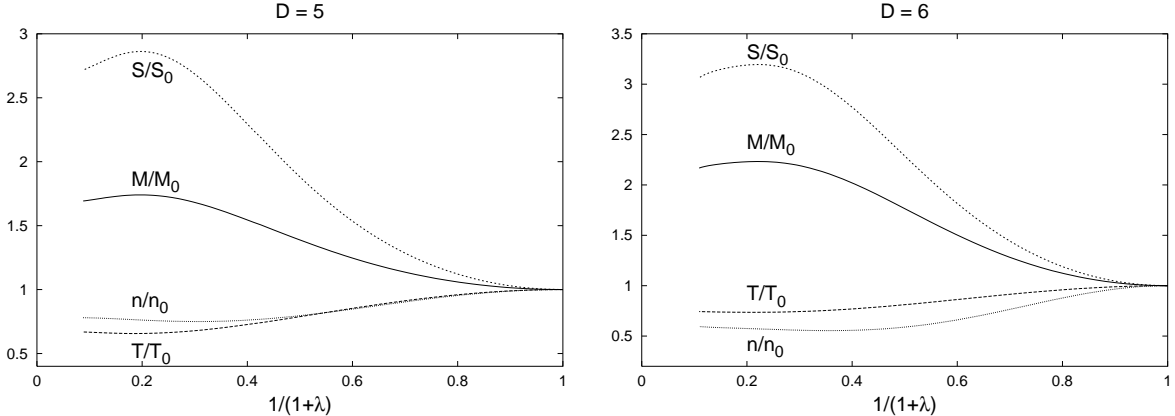


Figure 5. The M , the relative tension n , the temperature T and the entropy S of the $D = 5$ (a) and $D = 6$ (b) nonuniform string solutions are shown in units of the corresponding uniform string solution (denoted by M_0 , n_0 , T_0 , and S_0) as functions of $1/(1 + \lambda)$.

3.3 Black strings and black holes

In $D = 6$ dimensions, evidence was provided that the nonuniform string branch and the black hole branch merge at a topology changing solution [8]. We would now like to reconsider this evidence in the light of the continuation of the $D = 6$ nonuniform string branch to larger deformations, and further address the question, whether there is analogous evidence in $D = 5$ dimensions.

We therefore exhibit in Figure 6 the mass M versus the relative string tension n , for the nonuniform string branch as well as for the black hole branch in 5 and 6 dimensions. The black hole data are taken from [8]. First of all we note qualitative agreement of the shape and the relative position of the nonuniform string branch and the black hole branch in 5 dimensions with the shape and relative position of the corresponding branches in 6 dimensions. But compared to the data and discussion given in [8], we here observe a new feature: the backbending of the nonuniform string branch at a critical (minimal) value of the relative string tension n_b . Although the onset of this backbending can already be anticipated in the $D = 6$ data of [8]. But the backbending of the nonuniform string branch at n_b is still in accordance with the conjecture of a topology changing transition, occurring at $n_* > n_b$, both in 5 and 6 dimensions.

We attribute the presence of the gap between the black hole branch and the nonuniform string branch mainly to insufficient numerical data of the black hole branch close to the anticipated transition point. At such a transition point the nonuniform string parameter R_{\min} must approach zero (see Figure 4), and likewise the black hole parameter L_{axis} must approach zero, where L_{axis} measures the proper length along the exposed symmetry axis [8].

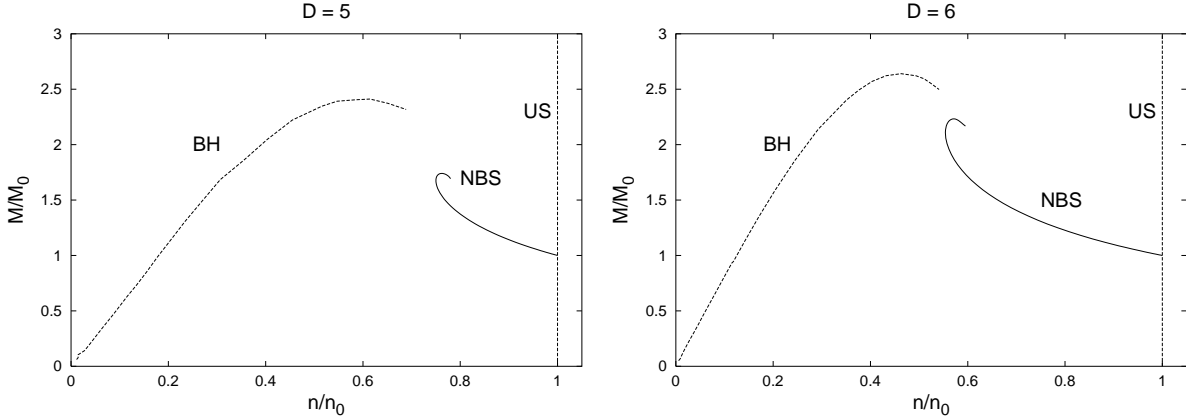


Figure 6. The mass M of the $D = 5$ (a) and $D = 6$ (b) nonuniform string and black hole branches is shown versus the relative string tension n . M and n are normalized by the values of the corresponding uniform string solutions. Here and in Figures 7-11, the data for the black hole branches is from [8].

We note, that close to the anticipated transition point, R_{\min} has decreased considerably farther (at the last numerically obtained point of the nonuniform string branch), than L_{axis} (at the last numerically obtained point of the black hole branch).

Since L_{axis} has decreased farther for $D = 6$ black holes than for $D = 5$ black holes, the gap between the branches is smaller in 6 dimensions than in 5 dimensions. We exhibit R_{\min} , R_{\max} , and L_{axis} as well as the black hole equatorial radius R_{eq} in Figure 7 for $D = 5$ and $D = 6$ solutions. R_{\min} and R_{\max} both exhibit the backbending feature present for nonuniform string solutions at large deformations. The figure is consistent with the vanishing of L_{axis} and R_{\min} at the same critical value of n . There R_{eq} and R_{\max} should also merge. The transition might then occur in the vicinity of $n_*/n_0 \approx 0.8$ for $D = 5$ and $n_*/n_0 \approx 0.6$ for $D = 6$ (as opposed to $n_b/n_0 \approx 0.55$ for $D = 6$, which was earlier assumed to be the transition point [8], but which is now realized to be the point where the backbending occurs). Extrapolating the black hole branch towards this critical value, the R_{eq} curve appears to smoothly reach the endpoint of the (backbending) upper part of the R_{\max} curve of the nonuniform string branch. The black hole data are again taken from [8].

Addressing the thermodynamic properties of the solutions, we exhibit in Figure 8 and Figure 9 the temperature and the entropy of $D = 5$ and $D = 6$ nonuniform strings and black holes. Extrapolating the black hole branch towards the critical value n_* , where the transition might occur, the black hole curves for temperature and entropy also appear to smoothly reach the endpoints of the corresponding (backbending) upper parts of the nonuniform string branch. This also holds for the mass, of course. Again, the black hole data are from [8].

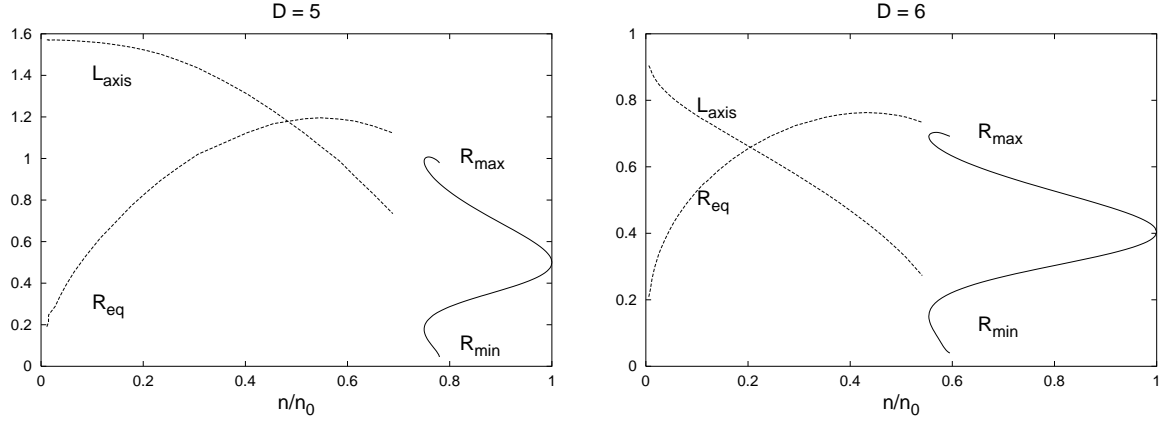


Figure 7. R_{min} , R_{max} , L_{axis} and R_{eq} of the $D = 5$ (a) and $D = 6$ (b) nonuniform string and black hole branches are shown versus the relative string tension n .

For very small masses localized black holes are entropically favoured, and for very large masses only uniform strings exist [8]. When the entropy is plotted versus the mass for the black hole branch and the uniform and nonuniform string branches, one observes, that the uniform strings become entropically favoured at a certain value of the mass, lying above the critical string mass and below the maximum black hole mass [8]. This is illustrated in Figure 10 for solutions in five and six dimensions.

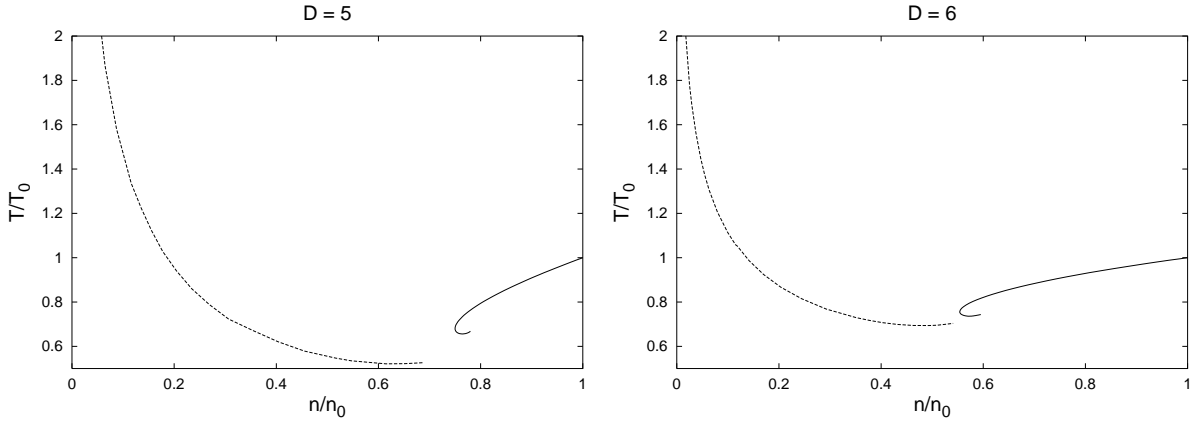


Figure 8. The temperature T of the $D = 5$ (a) and $D = 6$ (b) nonuniform string and black hole branches are shown versus the relative string tension n (in units of the uniform string quantities T_0 and n_0).

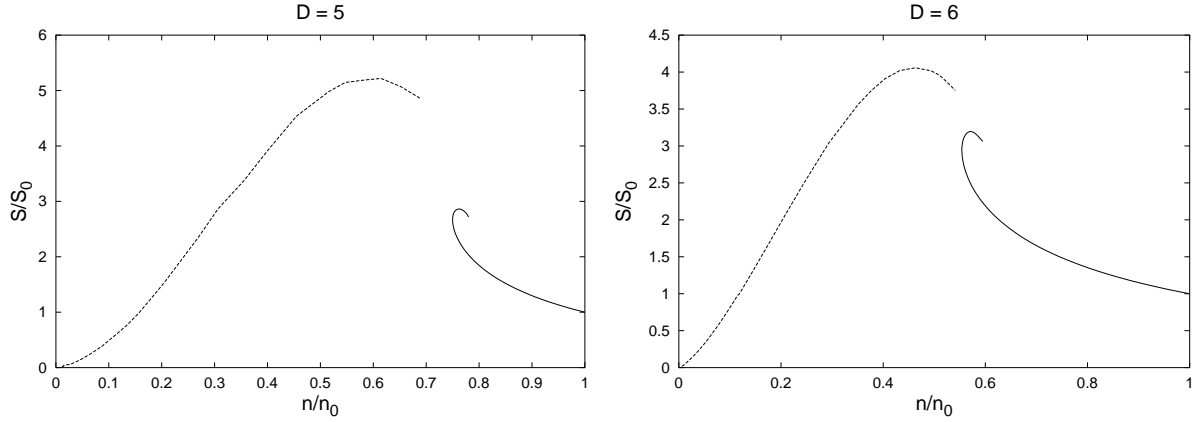


Figure 9. The the entropy S of the $D = 5$ (a) and $D = 6$ (b) nonuniform string and black hole branches are shown versus the relative string tension n (in units of the uniform string quantities S_0 and n_0).

Concluding, we observe qualitative agreement of all the physical properties of the solutions in 5 and in 6 dimensions. This strongly suggests, that the same phenomenon is present in both cases. In particular, all data are consistent with the conjecture that the black hole branch and the nonuniform string branch merge in a topology changing transition. Our new nonuniform string solutions give further credence to this scenario, but they still cannot confirm it.

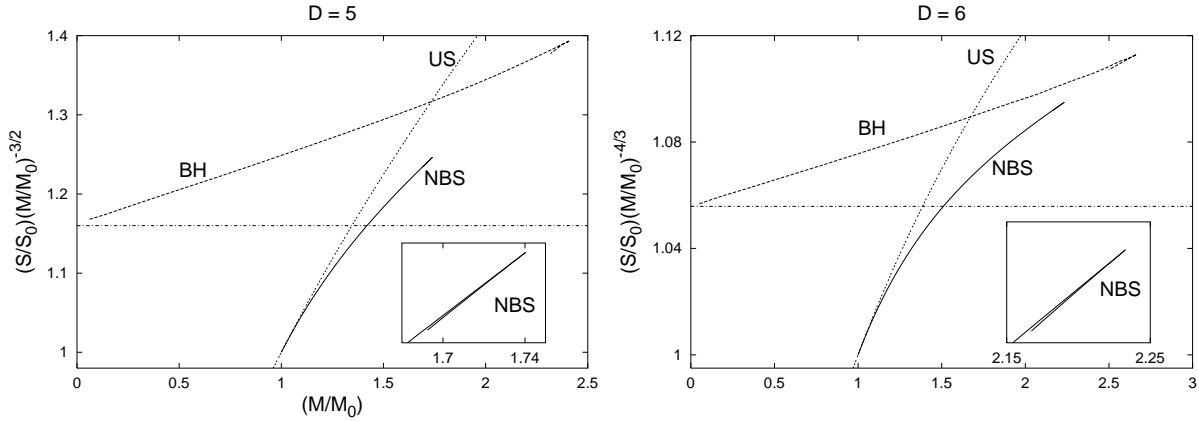


Figure 10. The product of entropy and mass $SM^{-3/2}$ (a) and $SM^{-4/3}$ (b) for the $D = 5$ (a) and $D = 6$ (b) nonuniform string branch, the uniform string branch and the black hole branch is shown as a function of the mass (in units of the corresponding critical string quantities). The horizontal lines represent the curves for the corresponding Schwarzschild-Tangherlini solutions.

4. Black string solutions in Einstein-Maxwell-dilaton theory

We now consider the action describing a gravitating Maxwell field coupled with a dilaton in a D -dimensional spacetime

$$I = \frac{1}{16\pi G} \int d^D x \sqrt{-g} \left(R - \frac{1}{2} g^{\mu\nu} \partial_\mu \phi \partial_\nu \phi - \frac{1}{4} e^{-2a\phi} F^2 \right), \quad (4.1)$$

where $F = dA$. The free parameter a governs the strength of the coupling of the dilaton to the Maxwell field.

The corresponding Einstein-Maxwell-dilaton (EMD) field equations are

$$\begin{aligned} R_{\mu\nu} - \frac{1}{2} R g_{\mu\nu} &= \frac{1}{2} T_{\mu\nu}, \\ \nabla^2 \phi &= -\frac{a}{2} e^{-2a\phi} F^2, \\ \partial_\mu (\sqrt{-g} e^{-2a\phi} F^{\mu\xi}) &= 0. \end{aligned} \quad (4.2)$$

with stress-energy tensor

$$\begin{aligned} T_{\mu\nu} &= T_{\mu\nu}^{(d)} + T_{\mu\nu}^{(em)}, \\ T_{\mu\nu}^{(d)} &= \partial_\mu \phi \partial_\nu \phi - \frac{1}{2} g_{\mu\nu} |\partial\phi|^2, \\ T_{\mu\nu}^{(em)} &= e^{-2a\phi} (F_{\mu\beta} F_{\nu\gamma} g^{\beta\gamma} - \frac{1}{4} g_{\mu\nu} F^2). \end{aligned} \quad (4.3)$$

Finding nonuniform black string and black hole solutions of these equations for a compact extradimension constitutes a formidable technical task. However, it appears possible to use the 'hidden' symmetries of the model (4.1) arising in the dimensionally reduced theory in order to generate nontrivial EMD solutions without actually solving the full set of equations.

This technique, known for the $D = 4$ Einstein-Maxwell theory since long, was generalized in the last years to higher dimensions and various other matter fields. In this paper, we'll follow the approach in [13], supposing the existence of one Killing vector $\partial/\partial y$, and write the D -dimensional line element in the form ³

$$ds^2 = g_{yy}(x) dy^2 + h_{ij}(x) dx^i dx^j, \quad (4.4)$$

performing the KK reduction with respect to the y -direction. As proven in [13], the reduced action corresponds to a non-linear σ -model, whose target space possesses a rich geometric structure. These symmetries imply the existence of a Harrison transformation nontrivially acting on the spacetime variables and matter fields. As a result, one may generate nontrivial

³Note that the Ref. [13] discusses a more general case, with an action principle containing a $(d+1)$ -differential form. Therefore, the general metric ansatz (4.4) will contain a set of d -coordinates y^i .

solutions of the D -dimensional EMD equations starting with known vacuum configurations. A detailed description of this procedure and the explicit form of the Harrison transformation is given in Ref. [13] (see also the results in [32]). This approach is valid for any value of the dilaton coupling constant (in particular also for Einstein-Maxwell theory, i.e., for $a = 0$, $\phi = 0$), and appears to be different from other results in literature. Ref. [33], for example, “charges up” the neutral KK solutions by uplifting them to eleven dimensional M-theory and employing boost and U-duality transformations, which fixes a particular value of the dilaton coupling constant a . The resulting solutions of type IIA/B string theory describe non-extremal p-branes on a circle.

Here we present only the resulting solutions, which have rather different properties, depending whether $\partial/\partial y$ is a timelike or spacelike Killing vector. Although the same generation techniques apply also for black hole solutions, we’ll restrict to the black string case.

4.1 Asymptotically $\mathcal{M}^{D-1} \times S^1$ EMD black string solutions

We start with a vacuum black string solution, written in the following form

$$ds^2 = -V(x)dt^2 + h_{ij}(x)dx^i dx^j. \quad (4.5)$$

where $\partial/\partial t$ is a timelike Killing vector.

The Harrison transformation in this case generates a one parameter family of black string solution in EMD theory, with line element

$$ds^2 = -V(\cosh^2 \beta - \sinh^2 \beta V)^{-2\alpha(D-3)} dt^2 + (\cosh^2 \beta - \sinh^2 \beta V)^{2\alpha} h_{ij} dx^i dx^j, \quad (4.6)$$

and matter fields

$$\begin{aligned} A_\mu &= \sqrt{2(D-2)\alpha} \frac{\tanh \beta e^{a\phi_0} V}{\cosh^2 \beta - \sinh^2 \beta V} \delta_{\mu t}, \\ \phi &= \phi_0 - 2a(D-2)\alpha \log(\cosh^2 \beta - \sinh^2 \beta V), \end{aligned} \quad (4.7)$$

where β , ϕ_0 are arbitrary real constants and

$$\alpha = (2a^2(D-2) + D-3)^{-1}. \quad (4.8)$$

For Einstein-Maxwell theory, we find $\alpha = 1/(D-3)$, the corresponding value in the Kaluza-Klein case being $\alpha = 1/(2(D-2))$.

Both uniform and nonuniform solutions of the EMD theory can be generated in this way. For example, the uniform string solution constructed within the metric ansatz (2.2) reads

$$\begin{aligned} ds^2 &= -\frac{f(r)}{(1 + (\frac{r_0}{r})^{D-4} \sinh^2 \beta)^{2\alpha(D-3)}} dt^2 + (1 + (\frac{r_0}{r})^{D-4} \sinh^2 \beta)^{2\alpha} \left(\frac{dr^2}{f(r)} + dz^2 + r^2 d\Omega_{D-3}^2 \right), \\ A_\mu &= \sqrt{2(D-2)\alpha} \frac{\tanh \beta e^{a\phi_0} f(r)}{1 + (\frac{r_0}{r})^{D-4} \sinh^2 \beta} \delta_{\mu t}, \\ \phi &= \phi_0 - 2a(D-2)\alpha \log\left(1 + \left(\frac{r_0}{r}\right)^{D-4} \sinh^2 \beta\right), \end{aligned} \quad (4.9)$$

For all a , the surface $r = r_0$ is an event horizon, while $r = 0$ is a curvature singularity. The extremal limit is found by taking $\beta \rightarrow \infty$ together with a rescaling of r_0 and has the form

$$ds^2 = -(1 + (\frac{c}{r})^{D-4})^{-2\alpha(D-3)} dt^2 + (1 + (\frac{c}{r})^{D-4})^{2\alpha} (\frac{dr^2}{f(r)} + dz^2 + r^2 d\Omega_{D-3}^2),$$

$$A_\mu = \frac{\sqrt{2(D-2)\alpha} e^{a\phi_0}}{1 + (\frac{c}{r})^{D-4}} \delta_{\mu t}, \quad \phi = \phi_0 - 2a(D-2)\alpha \log(1 + (\frac{c}{r})^{D-4}), \quad (4.10)$$

c being a real constant. Solutions describing several extremal black strings do also exist [20].

Returning to the general nonuniform string case, we observe that its relevant properties can be derived from the corresponding D -dimensional vacuum solution. The first thing to note is that the causal structure of the region $r > r_0$ is similar to the vacuum solutions; in particular one finds the same location of the event horizon. For the metric ansatz (2.2), the spacetime still approaches the $\mathcal{M}^{D-1} \times S^1$ background as $r \rightarrow \infty$, while the matter fields behave asymptotically as

$$A_t \simeq \Phi + \frac{Q_e}{r^{D-3}}, \quad \phi \simeq \phi_0 + \frac{Q_d}{r^{D-3}}, \quad (4.11)$$

where Q_e and Q_d correspond, in a suitable normalization, to the electric and the dilaton charges, respectively, Φ being the electrostatic potential difference between the event horizon and infinity,

$$\begin{aligned} \Phi &= \sqrt{2(D-2)\alpha} e^{a\phi_0} \tanh \beta, \\ Q_e &= -\sqrt{2(D-2)\alpha} e^{a\phi_0} \sinh \beta \cosh \beta c_t, \\ Q_d &= -2a\alpha(D-2) \sinh^2 \beta c_t. \end{aligned} \quad (4.12)$$

The mass \bar{M} , the string tension $\bar{\mathcal{T}}$ and the relative string tension \bar{n} of the EMD solutions are

$$\begin{aligned} \bar{M} &= M(1 + 2(D-3-n)\alpha \sinh^2 \beta), \\ \bar{\mathcal{T}} &= \mathcal{T}, \\ \bar{n} &= \frac{n}{1 + 2(D-3-n)\alpha \sinh^2 \beta}. \end{aligned} \quad (4.13)$$

The electric charge and the dilaton charge can also be expressed via (note also that the dilaton charge is not an independent quantity)

$$\begin{aligned} Q_e &= -\frac{M(D-3-n)}{(D-4)} \sqrt{\frac{\alpha}{2(D-2)}} e^{a\phi_0} \sinh 2\beta, \\ Q_d &= -\frac{2aM}{D-4} (D-3-n)\alpha \sinh^2 \beta. \end{aligned} \quad (4.14)$$

The relation between Hawking temperature \bar{T} and the entropy \bar{S} of the EMD solutions and the corresponding quantities T and S of the vacuum seed solution is

$$\bar{T} = T(\cosh \beta)^{-2\alpha(D-2)}, \quad \bar{S} = S(\cosh \beta)^{2\alpha(D-2)}, \quad (4.15)$$

thus the product TS remains invariant under the Harrison transformation.

The Smarr relation (2.15), derived in [17] for the vacuum case, admits a straightforward generalization to EMD theory,

$$\frac{D-3-n}{D-2}\bar{M} = \bar{T}\bar{S} - \frac{(D-3)(D-4)}{D-2}\Phi\tilde{Q}_e, \quad (4.16)$$

where $\tilde{Q}_e = \Omega_{D-3}LQ_e$. Therefore the thermodynamics of the EMD solutions can be derived from the vacuum solutions. When the parameter β is large one has a near extremal charged black string. However, a discussion of the extremal limit seems to require knowledge of the region $r < r_0$ of the seed metric.

We conclude that every vacuum solution is associated with a family of charged solutions, which depends on the parameter β . In particular, the branch of non-uniform solutions emerging from the uniform black string at the threshold unstable mode thus must persist for strings with non-zero electric charge. The fact that the ‘phase diagram’ of static solutions is qualitatively unchanged as the charge varies strongly suggests that there is still an instability for charged black strings [36, 35].

Also, a discussion of the thermodynamical properties of these solutions appears possible. This is interesting in connection with the Gubser-Mitra conjecture [34], that correlates the dynamical and thermodynamical stability for systems with translational symmetry and infinite extent. This conjecture has been discussed by several authors in the last years (see e.g. [35]-[37]). Ref. [35] uses the boost/duality transformation to map the phases of KK solutions onto phases of non- and near-extremal Dp-branes with a circle in their transverse space. The results there (see also [36]) confirm the validity of the Gubser-Mitra conjecture for non-extremal smeared branes. Similar conclusions are found in Ref. [37], where a discussion of thermodynamical stability of charged black p -branes within third-order perturbation theory is presented, the Gregory-Laflamme critical wavelength being also determined.

Asymptotically $\mathcal{M}^{D-1} \times S^1$ EMD black hole solutions can be generated by applying the same approach, starting with vacuum seed solutions written in the form (4.5). The resulting solutions are still given by (4.6)-(4.7), with the corresponding expressions of V , h_{ij} . Similar to the black string case, their properties are completely determined by the vacuum seed black hole solutions, the Smarr relation (4.16) being also satisfied.

4.2 Black strings in a background magnetic field

A rather different picture is found in the case when $\partial/\partial y$ in (4.4) is a spacelike Killing vector. Here we start with a vacuum black string solution (2.2) written in the form

$$ds^2 = -e^{2A(r,z)}f(r)dt^2 + e^{2B(r,z)}\left(\frac{dr^2}{f(r)} + dz^2\right) + e^{2C(r,z)}r^2(d\theta^2 + \sin^2\theta d\varphi^2 + \cos^2\theta d\Omega_{D-5}^2) \quad (4.17)$$

with $\theta \in [0, \pi/2]$, except for $D = 5$ where $\theta \in [0, \pi]$.

After applying a Harrison transformation to this configuration with respect to the Killing vector $\partial/\partial y \equiv \partial/\partial\varphi$, one finds the following solution of the EMD equations

$$ds^2 = \Lambda^{2\alpha}(r, z, \theta) \left(-e^{2A(r, z)} f(r) dt^2 + e^{2B(r, z)} \left(\frac{dr^2}{f(r)} + dz^2 \right) \right. \\ \left. + e^{2C(r, z)} r^2 (d\theta^2 + \cos^2 \theta d\Omega_{D-5}^2) \right) + \frac{e^{2C(r, z)} r^2 \sin^2 \theta}{\Lambda^{2\alpha(D-3)}(r, z, \theta)} d\varphi^2, \quad (4.18)$$

$$A_\mu(r, z, \theta) = \frac{B_0 e^{2C(r, z)} r^2 \sin^2 \theta}{\Lambda(r, z, \theta)} \delta_{\mu\varphi}, \quad (4.19)$$

$$\phi(r, z, \theta) = -\frac{2\alpha(D-2)}{2\alpha^2(D-2) + D-3} \log \Lambda(r, z, \theta), \quad (4.20)$$

where

$$\Lambda(r, z, \theta) = 1 + \frac{B_0^2 (2\alpha^2(D-2) + D-3)}{2(D-2)} e^{2C(r, z)} r^2 \sin^2 \theta, \quad (4.21)$$

B_0 is a free parameter which characterizes the central strength of the magnetic field, and α is still given by (4.8).

One can easily see that this solution is, in terms of the usual definitions, a black string, with an event horizon and trapped surfaces. Again, the causal structure of the solution is not affected by the Harrison transformation.

To clarify its asymptotics, we note that for $r \rightarrow \infty$, the line element (4.18) approaches the simpler form

$$ds^2 = \Lambda^{2\alpha} (-dt^2 + d\rho^2 + dz^2 + dz_1^2 + \dots + dz_{D-4}^2) + \Lambda^{-2\alpha(D-3)} \rho^2 d\varphi^2, \quad (4.22)$$

$$\Lambda = 1 + \frac{B_0^2}{2\alpha(D-2)} \rho^2,$$

where we introduced the new coordinates $\{\rho, z_1, \dots, z_{D-4}\}$ satisfying $r \cos \theta = (z_1^2 + \dots + dz_{D-4}^2)^{1/2}$, $r \sin \theta = \rho$, such that $[d(r \cos \theta)]^2 + (r \cos \theta)^2 d\Omega_{D-5}^2 = dz_1^2 + \dots + dz_{D-4}^2$.

Therefore, asymptotically the solution (4.18) approaches the Melvin fluxbrane found in [38], which represents a higher dimensional generalization of the four dimensional Melvin solution. The Melvin magnetic universe is a regular and static, cylindrically symmetric solution to Einstein-Maxwell(-dilaton) theory describing a bundle of magnetic flux lines in gravitational-magnetostatic equilibrium [39]. This solution has a number of interesting features, providing the closest approximation in general relativity for a uniform magnetic field. There exists a fairly extensive literature on the properties of this magnetic universe, of particular interest being the black hole solutions in universes which are asymptotically Melvin [40]. Black hole solutions in a higher dimensional Melvin universe have been constructed recently in [41].

Therefore, it is natural to interpret the EMD solution (4.18) as describing a black string in an external magnetic field. Note that, similar to the asymptotically $\mathcal{M}^{D-1} \times S^1$ case, one may generate also KK black hole solutions in a Melvin fluxbrane background.

One can compute the mass and tension of the black string solutions by using the background subtraction approach. In this case, the natural background is the Melvin solution (4.22). It follows that, different from the case of asymptotically $\mathcal{M}^{D-1} \times S^1$ solutions, these quantities are still given by (2.10). Moreover, it can be proven that the thermodynamic properties of the black string EMD solutions are unaffected by the external magnetic field, *i.e.* one finds the same expressions for the Hawking temperature and entropy as in the $B_0 = 0$ no magnetic field case. A similar property has been noticed in [42] for a $D = 4$ Schwarzschild black hole in a Melvin universe background (see also the $D > 4$ extensions [41]). Therefore, this seems to be a generic property of uncharged black hole/black string solutions in a background magnetic field extending to infinity. Heuristically, this is due to the fact that, in the static case, the mass-point/string source of these configurations does not interact directly with the background magnetic field.

5. Conclusions

Our first concern has been the numerical construction of $D = 5$ nonuniform strings, representing solutions of the vacuum Einstein equations. While their physical properties are similar to those of $D = 6$ nonuniform strings, their construction is more difficult. We attribute this to the slower asymptotic fall-off of the metric functions.

The branch of nonuniform strings emerges smoothly from the uniform string branch at the critical point, where its stability changes [1]. Keeping the horizon coordinate r_0 and the asymptotic length L of the compact direction fixed, the solutions depend on a single parameter, specified via the boundary conditions. Varying this parameter, the nonuniform strings become increasingly deformed, as quantified by the nonuniformity parameter λ . For the largest value of λ reached, the ‘waist’ of the string has a minimal radius of $R_{\min} \approx 0.1$ ($R_{\min} \approx 0.13$) for $\lambda = 9$ ($\lambda = 6$) in $D = 5$ ($D = 6$) dimensions, indicating that it is shrinking towards its asymptotic value of zero when $\lambda \rightarrow \infty$.

Previously, in $D = 6$ dimensions, evidence was provided that the nonuniform string branch and the black hole branch merge at a topology changing transition [8]. Although we see a backbending of the nonuniform string branch in both $D = 5$ and $D = 6$ dimensions, not observed previously, because the nonuniform string branch had not been continued to sufficiently high deformation, all our data are consistent with the assumption, that the nonuniform string branch and the black hole branch merge at such a topology changing transition. In fact, extrapolation of the black hole branch towards this transition point appears to match well the (extrapolated) endpoint of the (backbending) part of the nonuniform string branch.

For the phase diagram this would mean that we would have a region $0 < n < n_b$ with one branch of black hole solutions, then a region $n_b < n < n_*$ with one branch of black hole solutions and two branches of nonuniform string solutions, the ordinary one and the backbending one, and finally a region $n_* < n < n_0$ with only one branch of nonuniform string solutions. (We here do not address the bubble-black hole sequences present for $n > n_0$). Thus the topology changing transition would be associated with n_* , and $n_b < n < n_*$

would represent a middle region where three phases would coexist, one black hole and two nonuniform strings. This anticipated phase diagram is exhibited in Figure 11.

This is strongly reminiscent of the phase structure of the rotating black ring–rotating black hole system in $D = 5$ [43]. The (asymptotically flat) rotating black holes have S^3 horizon topology, and the (asymptotically flat) rotating black rings have $S^2 \times S^1$ horizon topology. The rotating black holes exist up to a maximal value of the angular momentum (for a given mass), $0 < J < J_*$, the rotating black rings are present only above a minimal value of the angular momentum (for a given mass), $J_b < J$, and in the middle region $J_b < J < J_*$ three phases coexist, one black hole and two black rings [43].

Further numerical work for nonuniform strings and in particular for black holes in the critical region close to n_* might confirm this picture further, and it might lead to further insight into the structure of the configuration space. The backbending of the nonuniform string branch clearly indicates that the configuration space is richer close to the anticipated

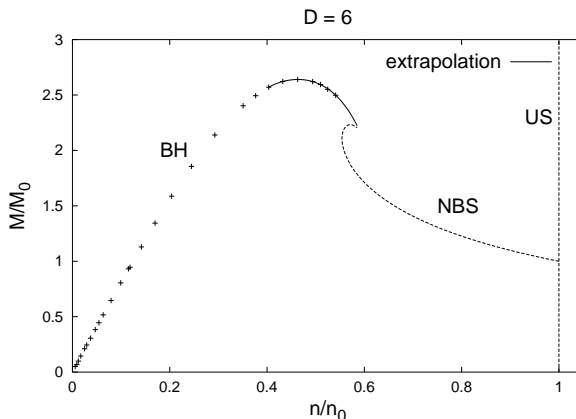


Figure 11. The mass M of the $D = 6$ nonuniform string and black hole branches is shown versus the relative string tension n . M and n are normalized by the values of the corresponding uniform string solutions. The black hole branch is extrapolated towards the anticipated critical value n_* .

topology changing transition, which currently still invites speculations [10, 44].

Our second concern has been the construction of black strings in EMD theory, obtained via a Harrison transformation. Different from other results in the literature (see e.g. [33]), the construction we proposed in Section 4 is valid for any value of the dilaton coupling constant. Apart from asymptotically $\mathcal{M}^{D-1} \times S^1$ charged black strings, we found also black string solutions in an external magnetic field. We found that the properties of these EMD configurations can be derived from the corresponding D -dimensional vacuum solution.

To push forward our understanding of these issues, it would be interesting to find both black hole and nonuniform black string branches for $D > 6$. The dimensions around $D = 13$ are of particular interest, since as found in [5], for $D > 13$ the perturbative nonuniform

strings are less massive than the uniform solutions. Moreover, their entropy is larger than the entropy of uniform strings with the same mass.

Acknowledgements

We are grateful to T. Wiseman for valuable discussions and for providing us with the $D = 5$ and $D = 6$ black hole data [8]. We would also like to thank D. H. Tchrakian for many useful discussions and comments. B.K. gratefully acknowledges support by the DFG under contract KU612/9-1. The work of E.R. was carried out in the framework of Enterprise-Ireland Basic Science Research Project SC/2003/390. This work is also supported by IC/05/03.

A. Appendix

As noted before for black holes, the most error prone part of the numerical procedure is the extraction of the mass M and the relative tension n from the asymptotic form of the metric via the coefficients c_t and c_z [4, 6, 8]. Whereas this extraction is quite accurate for nonuniform strings in 6 dimensions, it is quite problematic for nonuniform strings in 5 dimensions.

To see this we consider the asymptotic expansion for the metric functions in $D = 5$ dimensions.

$$A \rightarrow \frac{A_\infty}{r}, \quad B \rightarrow \frac{B_\infty}{r}, \quad C \rightarrow \frac{C_\infty \ln r}{r}, \quad (\text{A.1})$$

and in $D = 6$ dimensions

$$A \rightarrow \frac{A_\infty}{r^2}, \quad B \rightarrow \frac{B_\infty}{r^2}, \quad C \rightarrow \frac{C_\infty}{r}, \quad (\text{A.2})$$

In $D = 5$ the coefficients must satisfy $C_\infty = A_\infty + 2B_\infty$, a relation essential for the first law to hold.

In 6 dimensions the asymptotic fall-off is sufficiently fast, yielding excellent agreement for the mass and tension as obtained from the expansion coefficients with those obtained from the first law and the Smarr relation [6]-[8].

In 5 dimensions the numerical situation is much trickier, because of the presence of the log term in the function C . This is aggravated by the fact, that the coefficient C_∞ is an order of magnitude smaller than the other two coefficients. We therefore do not see the log dependence in the numerical results, when calculated in the full interval $[0 \leq \bar{r} \leq 1]$, $[0 \leq \bar{z} \leq 1]$. To observe the log dependence, we must switch to a system of ordinary differential equations after a certain value of \bar{r} , beyond which the \bar{z} -dependence has disappeared.

The coefficient c_t is nevertheless obtained with good accuracy, since it is associated with a conservation law, obtained from the equation for the metric function A Eq.(2.3), equivalent to the Smarr relation. The coefficient c_z , in contrast, is error prone, since the asymptotic fall-off of the function B is numerically not well determined.

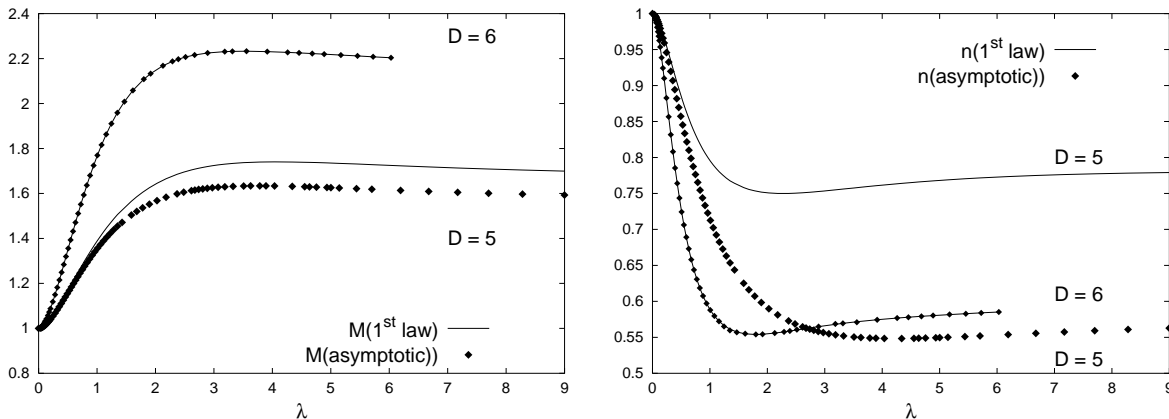


Figure 12. The mass M (a) and relative tension n (b) of the $D = 5$ and $D = 6$ nonuniform string branches are shown versus the nonuniformity parameter λ . The quantities are extracted from the first law and the Smarr relation, as well as from the asymptotic coefficients at $\bar{r} = 1$.

Reading off the values of the coefficient c_z at $\bar{r} = 1$ therefore leads to considerable disagreement of the values of the mass and tension with those values obtained from the first law and the Smarr relation. This is illustrated in Figure 12.

Our final remarks concern the numerical method and the quality of the solutions.

For the construction of the numerical solutions we use Newton-Raphson iteration. In each iteration step a correction to the initial guess configuration is computed. The maximum of the relative defect decreases by a factor of 20 from one iteration step to another. However, for large values of λ convergence is slower. In this case we re-iterate the solution until the defect is small enough (about 10^{-4}). Note, that this defect concerns the discretised equations. The estimates of the relative error of the solution (truncation error) are computed separately. They are of the order 0.001% for small λ , but increase up to 1% close to the backbending point. On the second branch the errors first decrease with increasing λ , but then increase again when the solutions become too steep at the waist. The errors also depend on the order of consistency of the method, i.e. on the order of the discretisation of derivatives. Usually 4th order gives reasonable results. For some solutions we used 6th order to check the consistency with the 4th order solutions.

We also monitored the violation of the constraints

$$C_1 = \sqrt{f}\sqrt{-g}(G_r^r - G_z^z), \quad C_2 = \sqrt{-g}G_z^z.$$

For small λ the maximum of the constraints is less than 0.1, but it increases with increasing λ . The maximum of the constraint C_2 is smaller by a factor of 5 compared to C_1 . On the second branch the maximum is of the order one. However, this large value appears in the vicinity of the waist ($z = L/2$ at the horizon), in a small region where the functions are extremely steep. Away from this region the violation of the constraints remains small. We also observed

that the condition $\partial B/\partial r = 0$ at the horizon is violated at the waist when λ becomes large. (A similar remark has been made in [4].) The violation of the condition $\partial B/\partial r = 0$ at the waist might be related to the violation of the constraints.

Increasing the number of grid points near $z = L/2$ yields smaller violation of the constraints and the condition $\partial B/\partial r = 0$ at the horizon. Also, the violation of the constraint C_1 is of the same magnitude as the maximum of the equations with the same weighting.

References

- [1] R. Gregory and R. Laflamme, Phys. Rev. Lett. **70** (1993) 2837 [arXiv:hep-th/9301052].
- [2] G. T. Horowitz and K. Maeda, Phys. Rev. Lett. **87** (2001) 131301 [arXiv:hep-th/0105111].
- [3] S. S. Gubser, Class. Quant. Grav. **19** (2002) 4825 [arXiv:hep-th/0110193].
- [4] T. Wiseman, Class. Quant. Grav. **20** (2003) 1137 [arXiv:hep-th/0209051].
- [5] E. Sorkin, Phys. Rev. Lett. **93** (2004) 031601 [arXiv:hep-th/0402216].
- [6] T. Wiseman, Class. Quant. Grav. **20** (2003) 1177 [arXiv:hep-th/0211028].
- [7] B. Kol and T. Wiseman, Class. Quant. Grav. **20** (2003) 3493 [arXiv:hep-th/0304070].
- [8] H. Kudoh and T. Wiseman, Phys. Rev. Lett. **94** (2005) 161102 [arXiv:hep-th/0409111].
- [9] B. Kol, JHEP **0510** (2005) 049 [arXiv:hep-th/0206220].
- [10] B. Kol, Phys. Rept. **422** (2006) 119 [arXiv:hep-th/0411240].
- [11] T. Harmark and N. A. Obers, arXiv:hep-th/0503020.
- [12] E. Sorkin, B. Kol and T. Piran, Phys. Rev. D **69** (2004) 064032 [arXiv:hep-th/0310096].
- [13] D. V. Gal'tsov and O. A. Rytchkov, Phys. Rev. D **58** (1998) 122001 [arXiv:hep-th/9801160].
- [14] G. W. Gibbons and S. W. Hawking, Phys. Rev. D **15** (1977) 2752.
- [15] T. Harmark and N. A. Obers, JHEP **0205** (2002) 032 [arXiv:hep-th/0204047].
- [16] J. H. Traschen and D. Fox, Class. Quant. Grav. **21** (2004) 289 [arXiv:gr-qc/0103106];
J. H. Traschen, Class. Quant. Grav. **21** (2004) 1343 [arXiv:hep-th/0308173].
- [17] T. Harmark and N. A. Obers, Class. Quant. Grav. **21** (2004) 1709 [arXiv:hep-th/0309116].
- [18] B. Kol, E. Sorkin and T. Piran, Phys. Rev. D **69** (2004) 064031 [arXiv:hep-th/0309190].
- [19] T. Harmark and N. A. Obers, JHEP **0405** (2004) 043 [arXiv:hep-th/0403103].
- [20] G. T. Horowitz, arXiv:hep-th/0205069.
- [21] T. Harmark and N. A. Obers, Nucl. Phys. B **684** (2004) 183 [arXiv:hep-th/0309230].
- [22] J. D. Brown and J. W. York, Phys. Rev. D **47** (1993) 1407.
- [23] P. Kraus, F. Larsen and R. Siebelink, Nucl. Phys. B **563** (1999) 259 [arXiv:hep-th/9906127];
S. R. Lau, Phys. Rev. D **60** (1999) 104034 [arXiv:gr-qc/9903038];
R. B. Mann, Phys. Rev. D **60** (1999) 104047 [arXiv:hep-th/9903229].

- [24] R. B. Mann and D. Marolf, arXiv:hep-th/0511096.
- [25] R. B. Mann and C. Stelea, Phys. Lett. B **634** (2006) 531 [arXiv:hep-th/0511180].
- [26] E. Witten, Nucl. Phys. B **195** (1982) 481.
- [27] F. Dowker, J. P. Gauntlett, G. W. Gibbons and G. T. Horowitz, Phys. Rev. D **52** (1995) 6929 [arXiv:hep-th/9507143];
O. Aharony, M. Fabinger, G. T. Horowitz and E. Silverstein, JHEP **0207** (2002) 007 [arXiv:hep-th/0204158].
- [28] D. Birmingham and M. Rinaldi, Phys. Lett. B **544** (2002) 316 [arXiv:hep-th/0205246];
V. Balasubramanian and S. F. Ross, Phys. Rev. D **66** (2002) 086002 [arXiv:hep-th/0205290].
- [29] H. Elvang, T. Harmark and N. A. Obers, JHEP **0501** (2005) 003 [arXiv:hep-th/0407050].
- [30] W. Schönauer and R. Weiß, J. Comput. Appl. Math. **27**, 279 (1989) 279;
M. Schauder, R. Weiß and W. Schönauer, The CADSOL Program Package, Universität Karlsruhe, Interner Bericht Nr. 46/92 (1992).
- [31] B. Kleihaus and J. Kunz, Phys. Rev. D **57** (1998) 834 [arXiv:gr-qc/9707045];
B. Kleihaus and J. Kunz, Phys. Rev. D **57** (1998) 6138 [arXiv:gr-qc/9712086];
B. Kleihaus, J. Kunz and F. Navarro-Lerida, Phys. Rev. D **66** (2002) 104001 [arXiv:gr-qc/0207042].
- [32] S. S. Yazadjiev, Phys. Rev. D **73** (2006) 064008 [arXiv:gr-qc/0511114].
- [33] T. Harmark and N. A. Obers, JHEP **0409** (2004) 022 [arXiv:hep-th/0407094].
- [34] S. S. Gubser and I. Mitra, arXiv:hep-th/0009126.;
S. S. Gubser and I. Mitra, JHEP **0108** (2001) 018 [arXiv:hep-th/0011127].
- [35] T. Harmark, V. Niarchos and N. A. Obers, JHEP **0510** (2005) 045 [arXiv:hep-th/0509011].
- [36] O. Aharony, J. Marsano, S. Minwalla and T. Wiseman, Class. Quant. Grav. **21** (2004) 5169 [arXiv:hep-th/0406210].
- [37] H. Kudoh and U. Miyamoto, Class. Quant. Grav. **22** (2005) 3853 [arXiv:hep-th/0506019].
- [38] G. W. Gibbons and K. i. Maeda, Nucl. Phys. B **298** (1988) 741.
- [39] M. A. Melvin, Phys. Lett. **8** (1964) 65.
- [40] W. A. Hiscock, J. Math. Phys. **22** (1981) 1828;
F. Ernst, J. Math. Phys. **17** (1976) 54.
- [41] M. Ortogio, JHEP **0505** (2005) 048 [arXiv:gr-qc/0410048].
- [42] E. Radu, Mod. Phys. Lett. A **17** (2002) 2277 [arXiv:gr-qc/0211035];
M. Agop, E. Radu and R. Slagter, Mod. Phys. Lett. A **20** (2005) 1077.
- [43] R. Emparan, H. S. Reall, Phys. Rev. Lett. **88** (2002) 101101 [arXiv:hep-th/0110260].
- [44] A possibility not excluded currently would be the presence of a spiral of nonuniform string solutions ending at n_* , as seen for instance for boson stars, see e.g. T. D. Lee and Y. Pang, Phys. Rept. **221** (1992) 251.